

1 **A method for continuous <sup>239</sup>Pu determinations in Arctic and Antarctic ice**  
2 **cores**

3 M. M. Arienzo<sup>1\*</sup>, J. R. McConnell<sup>1</sup>, N. Chellman<sup>1</sup>, A. S. Criscitiello<sup>2</sup>, M. Curran<sup>3,4</sup>, D.  
4 Fritzsche<sup>5</sup>, S. Kipfstuhl<sup>5</sup>, R. Mulvaney<sup>6</sup>, M. Nolan<sup>7</sup>, T. Opel<sup>5</sup>, M. Sigl<sup>8</sup>, J.P. Steffensen<sup>9</sup>

5 <sup>1</sup>Desert Research Institute, 2215 Raggio Parkway, Reno, NV, 33149, US

6 <sup>2</sup>University of Calgary, 2500 University Dr NW, Calgary, AB T2N 1N4, Canada

7 <sup>3</sup>Australian Antarctic Division, 203 Channel Highway, Kingston Tasmania 7050, Australia

8 <sup>4</sup>Antarctic Climate and Ecosystems Cooperative Research Centre, University of Tasmania,  
9 Hobart 7001, Australia.

10 <sup>5</sup>Alfred-Wegener-Institut, Potsdam/Bremerhaven, Germany

11 <sup>6</sup>British Antarctic Survey, High Cross, Madingley Road Cambridge, CB3 0ET, UK

12 <sup>7</sup>University of Alaska Fairbanks, 505 N Chandalar Dr, Fairbanks, AK, 99775, US

13 <sup>8</sup>Paul Scherrer Institute, 5232 Villigen, Switzerland

14 <sup>9</sup>Centre for Ice and Climate, Niels Bohr Institute, University of Copenhagen, Copenhagen,  
15 Denmark.

16 **CORRESPONDING AUTHOR**

17 \* Desert Research Institute, 2215 Raggio Parkway, Reno, NV, 33149, US; Email:  
18 marienzo@dri.edu; Phone: 775-673-7693

19

20

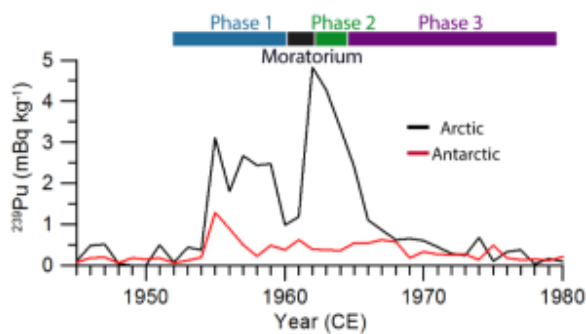
21

22

23 ABSTRACT

24 Atmospheric nuclear weapons testing (NWT) resulted in the injection of plutonium (Pu)  
25 into the atmosphere and subsequent global deposition. We present a new method for continuous  
26 semi-quantitative measurement of  $^{239}\text{Pu}$  in ice cores, which was used to develop annual records  
27 of fallout from NWT in ten ice cores from Greenland and Antarctica. The  $^{239}\text{Pu}$  was measured  
28 directly using an Inductively Coupled Plasma – Sector Field Mass Spectrometer, thereby  
29 reducing analysis time and increasing depth-resolution with respect to previous methods. To  
30 validate this method, we compared our one year averaged results to published  $^{239}\text{Pu}$  records and  
31 other records of NWT. The  $^{239}\text{Pu}$  profiles from four Arctic ice cores reflected global trends in  
32 NWT and were in agreement with discrete Pu profiles from lower latitude ice cores. The  $^{239}\text{Pu}$   
33 measurements in the Antarctic ice cores tracked low latitude NWT, consistent with previously  
34 published discrete records from Antarctica. Advantages of the continuous  $^{239}\text{Pu}$  measurement  
35 method are (1) reduced sample preparation and analysis time; (2) no requirement for additional  
36 ice samples for NWT fallout determinations; (3) measurements are exactly co-registered with all  
37 other chemical, elemental, isotopic, and gas measurements from the continuous analytical  
38 system; and (4) the long half-life means the  $^{239}\text{Pu}$  record is stable through time.

39 ABSTRACT ART



40

41 1. INTRODUCTION

42 The transuranic radioactive chemical element plutonium (Pu), first artificially produced in  
43 1940, is present in the environment as a result of nuclear weapons testing (NWT) conducted  
44 from 1945 to 1980 Common Era (CE).<sup>1</sup> Plutonium primarily exists as six isotopes: <sup>238</sup>Pu, <sup>239</sup>Pu,  
45 <sup>240</sup>Pu, <sup>241</sup>Pu, <sup>242</sup>Pu, and <sup>244</sup>Pu, with <sup>239</sup>Pu being the most abundant in the environment and <sup>244</sup>Pu  
46 having the longest half-life. It is estimated that 6.5 PBq of <sup>239</sup>Pu was released globally as a result  
47 of atmospheric NWT.<sup>1</sup>

48 Atmospheric nuclear weapons tests were primarily conducted in three major phases. Phase  
49 one occurred from 1952 to 1959 CE and was dominated by United States (U.S.) testing in the  
50 low latitude Pacific (Bikini, Eniwetok, and Johnston Islands) and in Nevada<sup>1</sup> (Figure 1). One of  
51 the largest tests conducted during this time was the Bravo test in February 1954 at Bikini Atoll,  
52 with a total yield of 15 Mt.<sup>1</sup> Other testing during this first period took place in the Pacific  
53 (Malden and Christmas Islands) and Australia by the United Kingdom (U.K.).<sup>1</sup> This period was  
54 followed by the Partial Test Ban moratorium from 1959 to 1961 CE. Phase two occurred from  
55 1961 to 1962 CE and was dominated by testing conducted by the former Soviet Union (USSR) at  
56 Novaya Zemlya (Russian Arctic) and Semipalatinsk (Kazakhstan) (Figure 1). The largest  
57 Northern Hemisphere (NH) testing occurred over the Russian Arctic during this period, with the  
58 yield accounting for ~57% of all atmospheric NWT.<sup>1,2</sup> Additional testing was conducted at the  
59 U.S. Pacific sites. In 1963 CE, the USSR and U.S. signed the Limited Test Ban Treaty in which  
60 the two countries stopped all aboveground testing. Phase three was dominated by  
61 aboveground tests from 1960 to 1980 CE largely conducted by France and China. French testing  
62 was conducted in the Algerian Sahara and French Polynesia (Mururoa and Fangataufa Atolls)

63 while Chinese testing primarily was conducted in Lop Nor, western China<sup>1</sup> (Figure 1).  
64 Radionuclide aerosols additionally were released during the Chernobyl accident in 1986 CE.<sup>2</sup>

65 Aerosols from NWT were dispersed on local, regional (tropospheric), or global  
66 (stratospheric) scales. Aerosols emitted by NWT were partitioned depending on the altitude and  
67 size of the test as well as the local meteorology,<sup>1</sup> and fallout occurred during periods ranging  
68 from minutes to five years following the atmospheric tests.<sup>3</sup> Aerosols injected into the  
69 stratosphere, which is thermally stratified from the troposphere, had the longest residence times.  
70 Radionuclides were transported in the atmosphere from testing sites to the high latitude ice cores  
71 sites in the stratosphere.<sup>4</sup> Radionuclides were transferred from the stratosphere to the troposphere  
72 seasonally, which in the NH occurred during the late winter to spring.<sup>4</sup> Removal of Pu from the  
73 atmosphere occurred either through wet (precipitation) or dry deposition,<sup>2</sup> and the greatest  
74 surface deposition of radionuclide aerosols was in the NH temperate latitudes with only 20% of  
75 the total fallout in the Southern Hemisphere (SH).<sup>5</sup>

76 Various chemical tracers have been utilized to reconstruct the transport and deposition of  
77 radionuclides associated with NWT (i.e., <sup>3</sup>H, <sup>14</sup>C, <sup>36</sup>Cl, <sup>90</sup>Sr, <sup>137</sup>Cs, <sup>210</sup>Pb, <sup>240</sup>Pu/<sup>239</sup>Pu, total-beta).  
78 Records of NWT have been developed from archives including vegetation and soil samples,<sup>4, 6</sup>  
79 corals,<sup>7, 8</sup> air filters,<sup>3, 9</sup> lake sediments,<sup>6, 10</sup> polar ice cores,<sup>2, 11-14</sup> and mid-latitude ice cores.<sup>15-19</sup>  
80 Proxies such as corals, lake sediments, and soils may exhibit post-depositional alteration, low  
81 accumulation, and mixing,<sup>6</sup> while ice cores typically exhibit higher annual accumulation rates  
82 and minimal post-depositional alteration or mixing. Ice cores have been successfully used to  
83 reconstruct atmospheric transport and fallout of NWT.<sup>2, 20</sup> Measurements of <sup>239</sup>Pu also have the  
84 potential to provide specific age tie points between various ice-core and other environmental  
85 records.<sup>11</sup>

86 The chemical content of ice cores is a proxy for atmospheric aerosol composition and  
87 therefore historical changes. Because of the long half-life of  $^{239}\text{Pu}$  (24.2 ky), the records of  $^{239}\text{Pu}$   
88 will be stable in ice cores through time, unlike beta-radiation-based methods. Due to the low  
89 concentration of Pu in the atmosphere and ice cores, sensitive instrumentation or large sample  
90 size is required for measurement. Traditional methods for analyzing Pu in ice cores include  
91 Accelerator Mass Spectrometry (AMS) which requires large dedicated sample sizes (hence  
92 reduced depth and temporal resolution, typically  $\sim 3$  years) and is time consuming both for  
93 sample preparation and analysis.<sup>16</sup> Gabrieli et al.<sup>15</sup> achieved higher resolution using semi-  
94 quantitative Inductively Coupled Plasma – Sector Field Mass Spectrometry (ICP-SFMS  
95 equipped with a desolvation nebulizer) measurements of  $^{239}\text{Pu}$  in discrete samples from an ice  
96 core from the Swiss/Italian Alps. These measurements yielded a time resolution of 0.5 to 1.5  
97 years while greatly reducing the time required for analysis.<sup>15</sup> Here we extend the ice core ICP-  
98 SFMS method from discrete to continuous, melter-based measurements using ICP-SFMS<sup>21</sup> –  
99 with the aim of minimizing sample requirements, sample handling, and decontamination efforts  
100 while maximizing depth resolution, measurement robustness and ensuring exact depth  
101 registration with all other chemical, elemental, isotopic, and gas measurements. We applied this  
102 new method to an array of ten annually dated ice cores from widely spaced sites both in  
103 Antarctica and Greenland (Figure 1) to develop an annual, semi-quantitative record of  $^{239}\text{Pu}$   
104 deposition throughout the high latitudes, and evaluate this new method through comparison to  
105 previously published discrete  $^{239}\text{Pu}$  records. We also demonstrated the usefulness of this new  
106 method as a dating tool by applying the method to three additional ice cores from Alaska, the  
107 Russian Arctic, and Antarctica with lower confidence depth-age scales.

## 108 2. MATERIAL AND METHODS

## 109 **2.1 Samples**

110 Four Arctic and six Antarctic ice cores were analyzed for semi-quantitative  $^{239}\text{Pu}$   
111 concentrations (Table 1, Figure 1). All ten cores previously had been dated using annual layer  
112 counting of multiple seasonal chemical cycles in the ice, and the dating was constrained with  
113 volcanic synchronization to the timescale of Sigl et al.<sup>22,23</sup> The Arctic cores included D4,<sup>24</sup>  
114 Summit\_2010, Tunu2013,<sup>22</sup> and NEEM-2011-S1<sup>22</sup> (Figure 1). The Antarctic cores are Aurora  
115 Basin North (ABN) and B40<sup>25</sup> from East Antarctica, James Ross Island<sup>26</sup> (JRI) from the  
116 Antarctic Peninsula, and Pine Island Glacier (PIG),<sup>27</sup> Thwaites Glacier (THW),<sup>27</sup> and the divide  
117 between Pine Island and Thwaites Glaciers (DIV)<sup>27</sup> from West Antarctica (Figure 1). Three  
118 additional ice cores from Alaska, the Russian Arctic, and Antarctica were also analyzed for  $^{239}\text{Pu}$   
119 and these samples consisted of lower confidence depth-age scales and will be discussed in detail  
120 in section 4.3.

## 121 **2.2 Analytical Methods**

122 Pu and a broad range of more than 20 elements and chemical species were analyzed using  
123 the Desert Research Institute's (DRI's) continuous melter system (adapted from McConnell et  
124 al.<sup>21</sup>) (Figure 2). For this study, methods and results will focus on  $^{238}\text{U}$  and  $^{239}\text{Pu}$ . Prior to  
125 analysis, longitudinal samples with a cross section of  $\sim 0.032$  by  $\sim 0.032$  m from all ice cores were  
126 cut and the ends decontaminated by scraping with a pre-cleaned ceramic knife.<sup>21, 28</sup> The ice cores  
127 were melted continuously from bottom to top and a portion of the meltwater from the  
128 uncontaminated center of the longitudinal sample was introduced to a Thermo-Finnigan  
129 Element2 (Thermo Scientific, Bremen, Germany) ICP-SFMS approximately four minutes after  
130 melting. The continuous sample stream was acidified inline to 2%  $\text{HNO}_3$ , with  $^{89}\text{Y}$  and  $^{115}\text{In}$   
131 added to the sample stream as external and internal standards, respectively (Figure 2). The ICP-  
132 SFMS was housed in a class-100 clean room, and the instrument outfitted with a cyclonic spray

133 chamber and a Teflon® PFA self-aspirating nebulizer (Elemental Scientific, Omaha, NE, USA)  
134 for stable sample introduction. The tubing from the melter into the ICP-SFMS was acid cleaned  
135 (1% HNO<sub>3</sub>) at least twice daily.

136 The ICP-MS instrument measured a suite of elements continuously in low resolution  
137 ( $M/\Delta M = 300$ )<sup>21</sup> (Figure 2). Therefore when conducting continuous elemental measurements of  
138 ice cores, there is an inherent tradeoff between temporal resolution of the analyses (i.e. ice core  
139 depth resolution) and measurement time spent on each element (Figure 2). With increased  
140 measurement time spent on each element, the number of measurements per element would  
141 increase, however the ice core depth resolution per element would decrease. This issue arises  
142 when conducting continuous Pu measurements. For <sup>239</sup>Pu measurements, the magnet was fixed at  
143 mass 238.050 with electric scanning (E-scan) between <sup>238</sup>U and <sup>239</sup>Pu. The <sup>239</sup>Pu sample time was  
144 0.4 s with 50 samples per peak (for 4 s total), and the <sup>238</sup>U sample time was 0.02 s with 50  
145 samples per peak. Overall, instrument measurement of all elements consisted of an effective  
146 sample rate of approximately 8 to 10 s (~6 mm sample depth). This approach allows for enough  
147 measurement time to be spent on Pu to acquire robust measurements while maintaining the ice  
148 core depth resolution for the additional elements. Ice core samples were not filtered, as particle  
149 influences are minimal. Every ~2.5 hours during routine pauses in the continuous ice-core  
150 analyses, procedural blanks were analyzed.

151 Similar to Gabrieli et al.,<sup>15</sup> we conducted an indirect calibration of <sup>239</sup>Pu utilizing <sup>238</sup>U.  
152 Five standards ranging in U concentration from 0.01 to 8.0 pg g<sup>-1</sup> were measured at the  
153 beginning of each analysis day with quality control standards analyzed at the beginning and end  
154 of the day. Standards were prepared from a 0.2 µg g<sup>-1</sup> multi-elemental stock solution (Inorganic  
155 Ventures, Christiansburg, VA, USA) in ultrapure 1% HNO<sub>3</sub>. Using the diluted standards, we

156 acquired a linear calibration curve and matrix matched the standards to the samples. As  
157 demonstrated by Gabrieli et al.,<sup>15</sup> this method provides a first approximation since the Pu and U  
158 ions behave similarly in the ICP-SFMS. From the semi-quantitative calibration, the <sup>239</sup>Pu results  
159 were expressed in concentration and activity units, using the <sup>239</sup>Pu specific activity value from  
160 Baglan et al.<sup>29</sup> of  $2.29 \times 10^9$  Bq g<sup>-1</sup>. Depositional flux of <sup>239</sup>Pu was calculated from <sup>239</sup>Pu activity  
161 multiplied by each year's water-equivalent accumulation derived from annual-layer counting.  
162 Since an indirect calibration was conducted <sup>239</sup>Pu concentration, activity and flux are semi-  
163 quantitative.

164 One potential source of interference for <sup>239</sup>Pu is <sup>238</sup>UH<sup>+</sup>.<sup>15</sup> As shown by Gabrieli et al.,<sup>15</sup>  
165 at low U concentrations (<40 pg g<sup>-1</sup>) the <sup>238</sup>UH<sup>+</sup> interferences were minimal and when  
166 interferences were detected, the interferences were much greater than <sup>239</sup>Pu measurements. In  
167 this study, the 1940 to 1985 CE average U concentration was ~0.25 pg g<sup>-1</sup> for the Greenland ice  
168 cores and ~0.05 pg g<sup>-1</sup> for the Antarctic ice cores. Additionally co-variability between Pu and U  
169 measurements was not observed for the Greenland or Antarctic ice cores between 1940 to 1985  
170 CE. While the U concentrations are low, to avoid potential <sup>238</sup>UH<sup>+</sup> interferences impacting results,  
171 the 4 s dwell for every 10 s sampling rate was averaged to one year intervals (~40 Pu  
172 measurements year<sup>-1</sup>) therefore reducing the measurement variability. To calculate the detection  
173 limit, blanks were analyzed periodically throughout the continuous analyses. The blank results  
174 were averaged to ~100 s intervals (~10 Pu measurements). The detection limit was then  
175 calculated as three times the standard deviation of the blanks with an average value of ~0.24 fg g<sup>-1</sup>  
176 (~0.55 mBq kg<sup>-1</sup>). After 60 s of blank washout, >90% of all U was removed, therefore memory  
177 effects are thought to be minimal. Blank correction was made by averaging the sample <sup>239</sup>Pu



178 value from 1900 to 1940 CE and subtracting from measured values. The average  $^{239}\text{Pu}$  for the ten  
179 ice cores from 1900 to 1940 CE was  $0.28 \text{ fg g}^{-1}$ .

### 180 3. RESULTS

181 Here we report continuous measurements of  $^{239}\text{Pu}$  from four Arctic and six Antarctic ice  
182 cores. All cores were previously dated with annual-layer counting with age uncertainties  
183 typically  $\leq 1$  year. The  $^{239}\text{Pu}$  data are presented as yearly averages. Composite records for  
184 concentration, activities, and fluxes were calculated from the geometric mean of the annual  
185 averages.

186 In the Arctic,  $^{239}\text{Pu}$  was first detected in the ice cores in 1953 CE, followed by a peak in  
187 1955 CE, a small decline in 1956 CE, and increased values to 1959 CE (Figure 3). The 1955 to  
188 1959 CE period consisted of an average  $^{239}\text{Pu}$  semi-quantitative concentration of  $1.1 \text{ fg g}^{-1}$  ( $2.5$   
189  $\text{mBq kg}^{-1}$ ). All ice cores exhibited a minimum from 1960 to 1961 CE, with an average  
190 concentration of  $0.5 \text{ fg g}^{-1}$  ( $1.1 \text{ mBq kg}^{-1}$ ). This was followed by a rapid increase in  $^{239}\text{Pu}$   
191 concentration from 1962 to 1965 CE, with average  $^{239}\text{Pu}$  values of  $1.6 \text{ fg g}^{-1}$  ( $3.7 \text{ mBq kg}^{-1}$ ), and  
192 the greatest  $^{239}\text{Pu}$  concentration ( $6.2 \text{ fg g}^{-1}$ ) was observed in the Tunu2013 ice core in 1962 CE.  
193 The  $^{239}\text{Pu}$  concentration significantly declined by 1968 CE, with values returning to background  
194 by  $\sim 1980$  CE. The average standard error of the measurement from 1945 to 1985 CE was  $0.2 \text{ fg}$   
195  $\text{g}^{-1}$ . Concentrations varied between sites because wet and dry deposition processes may have  
196 differed with accumulation rates and other depositional processes, therefore the  $^{239}\text{Pu}$  activity  
197 was converted to flux (Figure 3b). The D4 ice core had a greater accumulation rate and hence  
198 greater  $^{239}\text{Pu}$  activity flux than the other Arctic ice cores, with an average value of  $996 \text{ mBq m}^{-2}$   
199  $\text{yr}^{-1}$  from 1953 to 1965 CE (Figure 3b). The average  $^{239}\text{Pu}$  activity flux for the four Arctic ice  
200 cores from 1953 to 1965 CE was  $500 \text{ mBq m}^{-2} \text{ yr}^{-1}$ .

201 The semi-quantitative  $^{239}\text{Pu}$  activity measurements from six Antarctic ice cores are shown  
202 in Figure 4a. Overall,  $^{239}\text{Pu}$  levels were lower than those observed in the Arctic. Increased  
203 activities were observed from 1955 to 1957 CE (Figure 4a) with an average concentration of 0.4  
204  $\text{fg g}^{-1}$  ( $0.9 \text{ mBq kg}^{-1}$ ) and the greatest concentration ( $1.2 \text{ fg g}^{-1}$ ) measured in the THW core in  
205 1955 CE. After 1957 CE,  $^{239}\text{Pu}$  values declined followed by a peak in 1961 CE and a second  
206 peak from 1967 to 1968 CE and a return to background by  $\sim 1975$  CE. The average standard error  
207 of the measurement from 1945 to 1985 CE was  $0.1 \text{ fg g}^{-1}$  for the Antarctic ice cores. When  
208 accounting for accumulation rate variations, the greatest  $^{239}\text{Pu}$  flux was observed at the DIV,  
209 PIG, and THW cores, likely because of higher accumulation rate at these sites (Table 1, Figure  
210 4b) with an average  $^{239}\text{Pu}$  flux of  $250 \text{ mBq m}^{-2} \text{ yr}^{-1}$  from 1953 to 1965 CE. The average Antarctic  
211  $^{239}\text{Pu}$  flux for the six ice cores was  $120 \text{ mBq m}^{-2} \text{ yr}^{-1}$  from 1953 to 1965 CE.

## 212 4. DISCUSSION

### 213 4.1 Comparison to published NWT records

214 To evaluate the  $^{239}\text{Pu}$  measurements, we compared composite ice-core records of  $^{239}\text{Pu}$   
215 activity to published total NWT fission yields<sup>1</sup> (Figure 5). The first significant atmospheric tests  
216 were conducted in 1952 CE and included the Mike test in Eniwetok Atoll and the 1955 CE  
217 Bravo test.<sup>1</sup> These tests were reflected in both the Arctic and Antarctic ice cores with the first  
218 detection of  $^{239}\text{Pu}$  in 1953 CE and increased  $^{239}\text{Pu}$  from 1955 to 1959 CE dominated by the U.S.  
219 tests in the low-latitude Pacific. With the largest tests conducted from 1952 to 1958 CE.<sup>1</sup> The  
220 Partial Test Ban moratorium resulted in a decline in  $^{239}\text{Pu}$ , but values remained above baseline.  
221 This has been shown in other ice cores<sup>15</sup> and is thought to be due to the longer residence time of  
222  $^{239}\text{Pu}$  in the atmosphere. Post-moratorium in the fall of 1961 CE, the USSR resumed tests  
223 corresponding to a period of the most powerful testing, particularly at the Novaya Zemlya site  
224 with a test in October 1961 CE with a total release of 50 Mt.<sup>1</sup> This increase in testing clearly was

225 reflected in the Arctic record, with the greatest measured values during the post-moratorium  
226 (post-1961 CE) period. Unlike the Arctic, where the peak  $^{239}\text{Pu}$  concentration measurement  
227 occurred during the early 1960s, after 1958 CE the Antarctic  $^{239}\text{Pu}$  record remained relatively  
228 low, with only a slight increase in the early and late 1960s. Although the tests conducted in the  
229 1960s were large, there was minimal transport from the Russian Arctic to Antarctica, hence the  
230 low  $^{239}\text{Pu}$ . In 1963 CE, the Limited Test Ban Treaty was signed and  $^{239}\text{Pu}$  activity in both the  
231 Arctic and Antarctic records began to decline. Activity remained above baseline, however, as  
232 French and Chinese testing continued into the late 1970s. French testing in the South Pacific  
233 Ocean in Fangataufa and Mururoa Islands peaked in 1968 CE, which was reflected in our  
234 Antarctic records (Figure 5).

235 From 1953 to 1980 CE, more than 500 aboveground nuclear weapons tests resulted in  
236 global fallout of  $^{239}\text{Pu}$ . With most of the testing conducted in the NH, the NH to SH ratio of  $^{239}\text{Pu}$   
237 fallout<sup>4</sup> was  $\sim 3:1$ , and similarly the average  $^{239}\text{Pu}$  activity for the Arctic and Antarctic ice cores  
238 was  $1.3$  and  $0.4$   $\text{mBq kg}^{-1}$ , respectively.

#### 239 **4.2 Comparison to previously published records of fallout**

240 We performed further evaluation of the continuous  $^{239}\text{Pu}$  method by comparing the  
241 Antarctic and Arctic composite records to previously published discrete  $^{239}\text{Pu}$  records. When  
242 comparing to various ice-core records, overall good agreement was observed – expected given  
243 that NWT aerosols were globally distributed – and provided greater confidence in the method  
244 (Figure 6). Results from three Greenland sites (South Dome, Camp Century, and Dye-3) showed  
245 increased  $^{239}\text{Pu}$  from 1955 to 1960 CE with greater values from 1963 to 1965 CE.<sup>11, 30, 31</sup> The  
246 1965 CE  $^{239}\text{Pu}$  activity from South Dome<sup>30, 32</sup> was  $9 \pm 0.3$  d.p.h.  $\text{kg}^{-1}$ , similar to the average  
247 activity of  $2.4$   $\text{mBq kg}^{-1}$  observed in Greenland from this study. The average value at Camp

248 Century<sup>32</sup> for the 1965 CE stratum, however, was higher at  $11.3 \pm 0.3$  d.p.h.  $\text{kg}^{-1}$ , potentially  
249 because of variations in flux. The <sup>239</sup>Pu post-moratorium (1962 to 1965 CE) to pre-moratorium  
250 (1955 to 1959 CE) ratio was 59:41% for Dye-3, 56:44% for South Dome,<sup>31</sup> and 60:40% for this  
251 study. These ratios were offset from the 70:30% determined from the total atmospheric NWT,  
252 possibly due to variations in the type of weapons tested,<sup>31</sup> transport, or depositional processes.

253 With respect to lower latitude records, the Colle Gnifetti and Colle du Dome from the  
254 Alps both show two <sup>239</sup>Pu peaks in the pre-moratorium period (1955 to 1959 CE) with a  
255 minimum in 1957 CE,<sup>15</sup> similar to the observations in the Arctic records (Figure 6). The records  
256 from UK herbarium specimens,<sup>4</sup> and ice cores from Belukha Glacier,<sup>16</sup> Colle Gnifetti,<sup>15</sup> and  
257 Colle du Dome<sup>4</sup> all demonstrate increased <sup>239</sup>Pu activity post-moratorium (post-1961 CE).

258 Few studies have been conducted on Antarctic ice cores, but we observed generally  
259 favorable agreement with discrete <sup>239</sup>Pu records from Antarctica. The <sup>239</sup>Pu record from the Ross  
260 Ice Shelf showed a similar trend to the Antarctic ice-core records presented here, with the  
261 greatest <sup>239</sup>Pu values observed from 1952 to 1955 CE ( $\sim 8$  d.p.h.  $\text{kg}^{-1}$ ),<sup>33</sup> slightly higher than the  
262 peak values observed in this study. This was followed by a <sup>239</sup>Pu activity peak of about half the  
263 size from 1962 to 1966 CE attributed to USSR and U.S. testing and an increase in the early  
264 1970s attributed to French low-latitude testing.<sup>33</sup> Similar observations were made at Dome C  
265 with a large increase in <sup>239</sup>Pu observed in 1956 CE ( $34 \pm 0.8$  d.p.h.  $\text{kg}^{-1}$ ) and significantly lower  
266 levels in the 1960s.<sup>34</sup> The <sup>239</sup>Pu activity record from Dome C was greater than those observed  
267 here, but displayed a very similar overall trend.<sup>32-34</sup> The post-moratorium (1962 to 1965 CE) to  
268 pre-moratorium (1955 to 1959 CE) ratio for <sup>239</sup>Pu was 36:64 % for Dome C, 57:43 % for the  
269 Ross Ice Sheet,<sup>31</sup> and for this study was 38:62 % (Figure 6).

#### 270 **4.3 Application of the continuous <sup>239</sup>Pu method**

271           Considering the favorable comparison between the well-dated ice cores to previously  
272 published discrete records, we applied our method to ice cores with lower confidence depth-age  
273 scales and compared the measurements to the Arctic and Antarctic  $^{239}\text{Pu}$  composite records  
274 (Figure 7). Three additional cores were analyzed for  $^{239}\text{Pu}$  from sites where very low snow  
275 accumulation and/or surface melting and percolation result in less distinct annual chemical  
276 cycles and so lower confidence depth-age scales (Table 1). These additional cores included  
277 McCall Glacier (McCallUC) from the Brooks Range, Alaska,<sup>35</sup> Akademii Nauk<sup>36</sup> from the  
278 Russian Arctic, and a Norwegian/U.S. (NORUS) traverse core Site 8\_5 from East  
279 Antarctica<sup>37</sup>(Figure 1).

280           The Akademii Nauk results from Severnaya Zemlya (Russian Arctic), located in close  
281 proximity to the Russian Novaya Zemlya test site (Figure 1), showed increased  $^{239}\text{Pu}$  from 1953  
282 to 1958 CE, with a peak value of  $16 \text{ mBq kg}^{-1}$  in 1955 CE and no  $^{239}\text{Pu}$  increase in the post-  
283 moratorium period (Figure 7b). This was similar to the  $^{210}\text{Pb}$  measurements on the same ice core  
284 (Figure 7b) which showed a peak from 1953 to 1956 CE.<sup>12</sup> This is in contrast to the  $^{137}\text{Cs}$  activity  
285 measurements from Akademii Nauk which peaked from 1962 to 1965 CE with a smaller increase  
286 from 1953 to 1955 CE, in agreement with NWT records<sup>12</sup> (Figure 7b). The Austfonna ice core  
287 record from Svalbard, sampled at a 3-5 year resolution, also contained one significant  $^{239}\text{Pu}$  peak  
288 from 1956 to 1959 CE (Figure 6b). Considering the low Pu sampling resolution of the Austfonna  
289 ice core record from Svalbard, care must be taken when interpreting this core. However,  
290 previous studies propose that the deeper  $^{239}\text{Pu}$  from Austfonna<sup>2</sup> and the deeper  $^{210}\text{Pb}$  peak in  
291 Akademii Nauk<sup>12</sup> are due to the percolation and migration of  $^{239}\text{Pu}$  and  $^{210}\text{Pb}$  during melt  
292 periods.<sup>2, 12, 36</sup> This interpretation is potentially supported by the  $^{239}\text{Pu}$  measurements presented  
293 here. Alternatively, the electrical conductivity and sulfate records for Akademii Nauk exhibited a

294 sharp increase at 1956 CE thought to be associated with the Bezymianny volcanic eruption.<sup>36</sup>  
295 This suggests that the <sup>210</sup>Pb and <sup>239</sup>Pu records in Akademii Nauk may be impacted by dust  
296 deposited during the volcanic event.<sup>36</sup> These results demonstrate that an ice core with high melt  
297 and high amount of volcanic deposits may impact the <sup>239</sup>Pu record.

298 The <sup>239</sup>Pu record from McCallUC consisted of the greatest <sup>239</sup>Pu activity measured  
299 (Figure 7c). <sup>239</sup>Pu was initially detected in 1946 CE and steadily increased to a peak in 1956 CE  
300 of 13.6 mBq kg<sup>-1</sup>. This was followed by a decline in 1957 CE and a second peak in 1959 CE.  
301 Post-1961, <sup>239</sup>Pu activities increased to 19 mBq kg<sup>-1</sup> in 1964 CE. Values in the McCallUC record  
302 remained elevated until 1980 CE, when values returned to baseline. While the <sup>239</sup>Pu activity was  
303 much greater in McCallUC than found in the other cores analyzed here, the overall pattern was  
304 similar to observed Greenland records, verifying the depth-age scale (Figure 7). The post-  
305 moratorium (1962 to 1965 CE) to pre-moratorium (1955 to 1959 CE) ratio for <sup>239</sup>Pu was 59:41%  
306 for McCallUC, also similar to the Greenland records. The McCallUC site is a high dust site  
307 potentially influenced by high northern latitude mining operations. Therefore, the greater <sup>239</sup>Pu  
308 activities measured in the McCallUC record may be impacted by the deposition of crustal dust  
309 material contaminated with <sup>239</sup>Pu or <sup>238</sup>U, suggesting that care must be taken when applying this  
310 method in high dust localities.<sup>15</sup>

311 The NORUS site 8\_5 is a site of very low accumulation, however the <sup>239</sup>Pu results agreed  
312 well with the composite Antarctic record providing confidence in the age dating of this core. The  
313 <sup>239</sup>Pu record showed increased semi-quantitative <sup>239</sup>Pu activity from 1953 to 1956 CE and lower  
314 <sup>239</sup>Pu activity post-moratorium (Figure 7d). The semi-quantitative <sup>239</sup>Pu activity was much  
315 greater than that measured at the other Antarctic sites due to the low accumulation rate (Table 1).

316 When accounting for variations in snowfall rates, the 1955 CE  $^{239}\text{Pu}$  activity flux was 130 mBq  
317  $\text{m}^{-2}\text{yr}^{-1}$  for site 8\_5, lower than the average 277  $\text{mBq m}^{-2}\text{yr}^{-1}$  observed in Antarctica.

#### 318 **4.4 Environmental application**

319 These results demonstrate the capabilities of the continuous ICP-SFMS  $^{239}\text{Pu}$  method  
320 when applied to ice cores. Here we produced two high latitude composite records of  $^{239}\text{Pu}$   
321 applicable to the future evaluation and synchronization of ice cores chronologies, particularly for  
322 hard to date ice cores. While this method should be used with caution in high dust regions  
323 because of isobaric interferences from high U levels, our method for semi-quantitative  $^{239}\text{Pu}$   
324 determinations provides an age constraint without the need for additional ice analyses. The  
325 continued application of this new method to a wide range of ice cores from varying localities  
326 may additionally shed light on lower latitude atmospheric aerosol sources and transport  
327 processes to the high latitudes.

#### 328 **FIGURE CAPTIONS**

329 Figure 1: Ice cores analyzed in this study with well-constrained ages are shown as circles; ice  
330 cores with less constrained ages are shown as triangles. Black squares are  $^{239}\text{Pu}$  records  
331 previously published from U.K. herbarium samples,<sup>4</sup> and ice cores from Austfonna,<sup>2</sup> Colle du  
332 Dome near Mont Blanc,<sup>4</sup> Colle Gnifetti,<sup>15</sup> and Belukha Glacier.<sup>16</sup> Crosses indicate sites with  
333 significant NWT.<sup>1</sup>

334 Figure 2: Schematic of the ice-core melter, ICP-SFMS (left) and continuous flow analysis<sup>21</sup>  
335 (CFA) (right) systems, with examples of the types of elements and chemical species analyzed.  
336 The water pumped to the ICP-SFMS is from the center of the ice, and the flow path to both ICP-  
337 SFMS instruments is highlighted in red.

338 Figure 3: Annual average  $^{239}\text{Pu}$  results from the Arctic ice cores with well-constrained ages. (a)  
339 Semi-quantitative  $^{239}\text{Pu}$  activities and (b) semi-quantitative  $^{239}\text{Pu}$  activity fluxes for each of the  
340 ice cores with the composite geometric mean in black.

341 Figure 4: Annual average  $^{239}\text{Pu}$  results from the Antarctic ice cores with well-constrained ages.  
342 (a) Semi-quantitative  $^{239}\text{Pu}$  activities and (b) semi-quantitative  $^{239}\text{Pu}$  activity fluxes for each of  
343 the ice cores with the composite geometric mean in black.

344 Figure 5: Arctic (black) and Antarctic (red) composite semi-quantitative  $^{239}\text{Pu}$  activity compared  
345 to total NWT fission yields.<sup>1</sup> The NWT fission yields are divided by country and location of  
346 testing. Error bars represent the standard error of the mean.

347 Figure 6: Comparison to previously published  $^{239}\text{Pu}$  records. (a) Arctic mean (this study) (black),  
348 (b)  $^{239}\text{Pu}$  activity from Austfonna ice core (purple),<sup>2</sup> (c) Belukha Glacier ice core (light blue)<sup>16</sup>,  
349 (d) herbarium samples collected in the U.K. (green),<sup>4</sup> (e) Colle du Dome ice core (orange),<sup>4</sup> (f)  
350 Colle Gnifetti ice core (blue),<sup>15</sup> and (g) Antarctic composite (this study) (red). Note the Colle du  
351 Dome  $^{239}\text{Pu}$  activity record is plotted on its own depth scale. Error bars are standard error of the  
352 mean.

353 Figure 7: Comparison between  $^{239}\text{Pu}$  activity records from well-dated ice cores and ice cores  
354 with less constrained age scales. (a) Arctic composite record, (b) Akademii Nauk ice core  $^{239}\text{Pu}$   
355 activity (green), (c) McCallUC ice core (blue), (d) the Antarctic NORUS site 8\_5 (purple), and  
356 (e) the Antarctic composite. Also shown are the Akademii Nauk  $^{210}\text{Pb}$  activity (orange) and  $^{137}\text{Cs}$   
357 activity (brown) measurements from Pinglot et al.<sup>12</sup> Error bars are standard error of the mean.

358

359



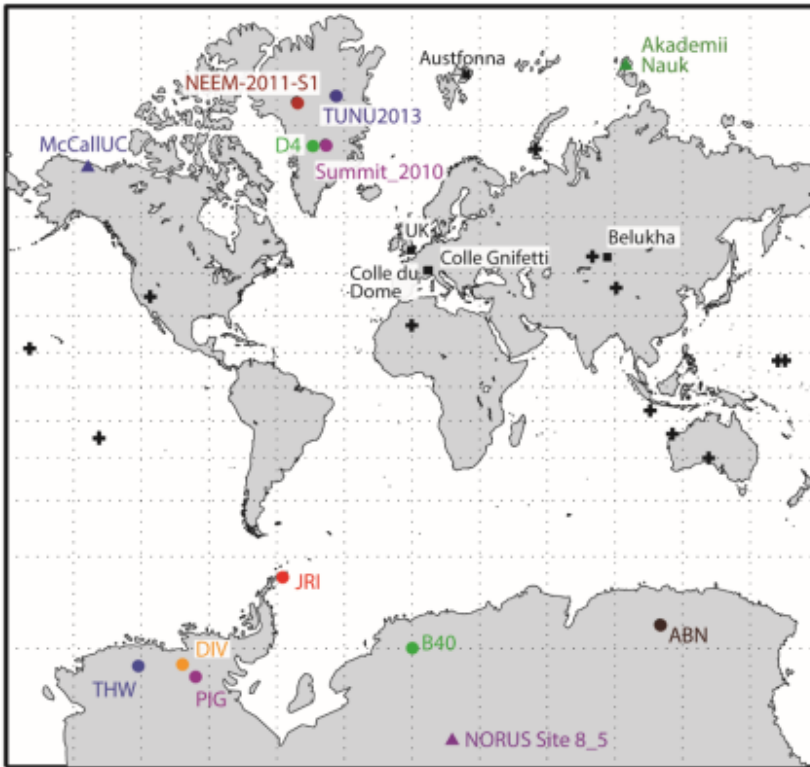
## 360 TABLES AND FIGURES

Site	Latitude (deg)	Longitude (deg)	Recent Accumulation kg m <sup>-2</sup> y <sup>-1</sup>
D4	71°24' N	43°54' W	414
NEEM_2011_S1	77° 26' 56" N	51° 03' 22" W	204
Summit 2010	72° 36' N	38° 18' W	221
Tunu2013	78° 2' N	33° 52' W	112
Akademii Nauk*	80° 31' N	94° 49' E	423
McCallUC*	69° 18' N	143° 48' W	546
ABN	72° 00' S	110° 00' E	109
B40	75° 0' S	0°3'36" E	68
DIV	76° 46' 13" S	101° 44' 15" W	372
JRI	64° 12' S	57° 42' W	595
PIG	77° 57' 25" S	95° 57' 42" W	400
THW	76° 57' 9" S	121° 13' 13" W	274
Site_8_5*	82° 38' S	17° 52' E	35

361

362 Table 1: Arctic and Antarctic sites used in this study. \*Indicates records with lower confidence  
363 depth-age scales.

364



365

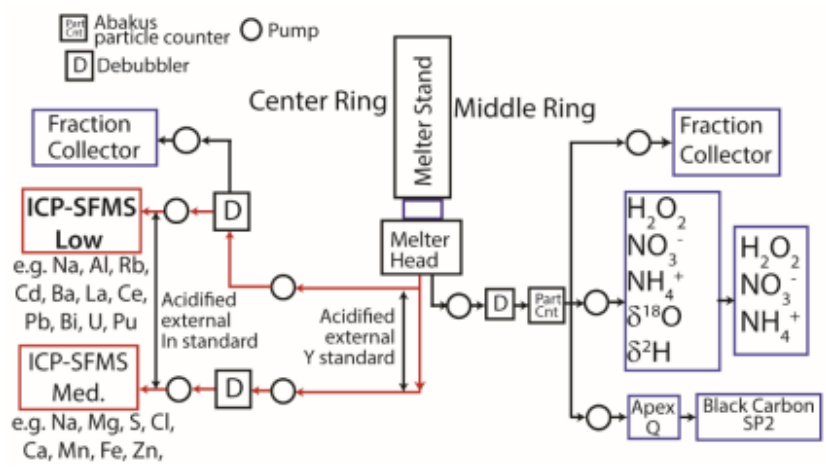
366 Figure 1: Ice cores analyzed in this study with well-constrained ages are shown as circles; ice  
 367 cores with less constrained ages are shown as triangles. Black squares are  $^{239}\text{Pu}$  records  
 368 previously published from U.K. herbarium samples,<sup>4</sup> and ice cores from Austfonna,<sup>2</sup> Colle du  
 369 Dome near Mont Blanc,<sup>4</sup> Colle Gnifetti,<sup>15</sup> and Belukha Glacier.<sup>16</sup> Crosses indicate sites with  
 370 significant NWT.<sup>1</sup>

371

372

373

374

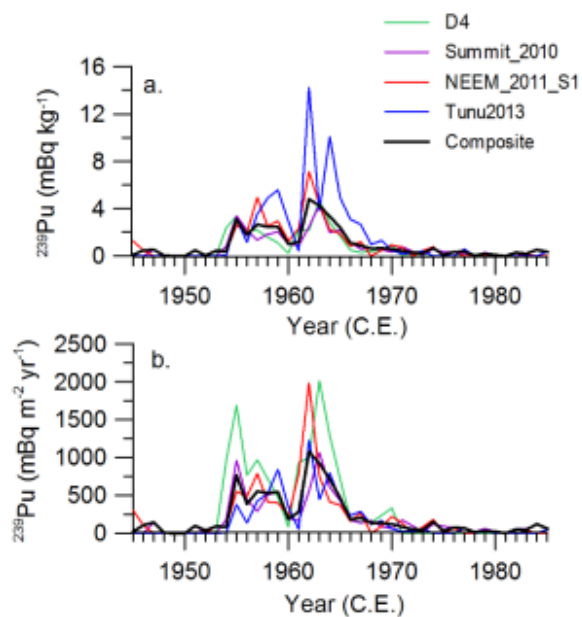


375

376 Figure 2: Schematic of the ice-core melter, ICP-SFMS (left) and continuous flow analysis<sup>21</sup>  
 377 (CFA) (right) systems, with examples of the types of elements and chemical species analyzed.  
 378 The water pumped to the ICP-SFMS is from the center of the ice, and the flow path to both ICP-  
 379 SFMS instruments is highlighted in red.

380

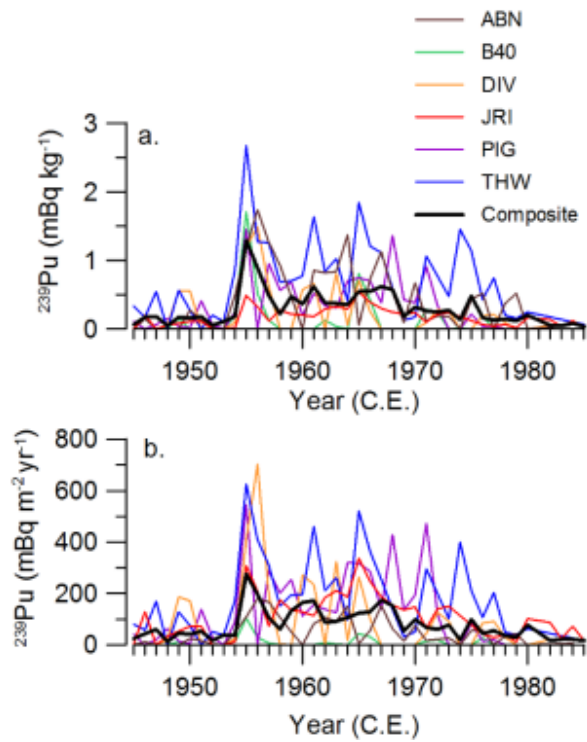
381



382

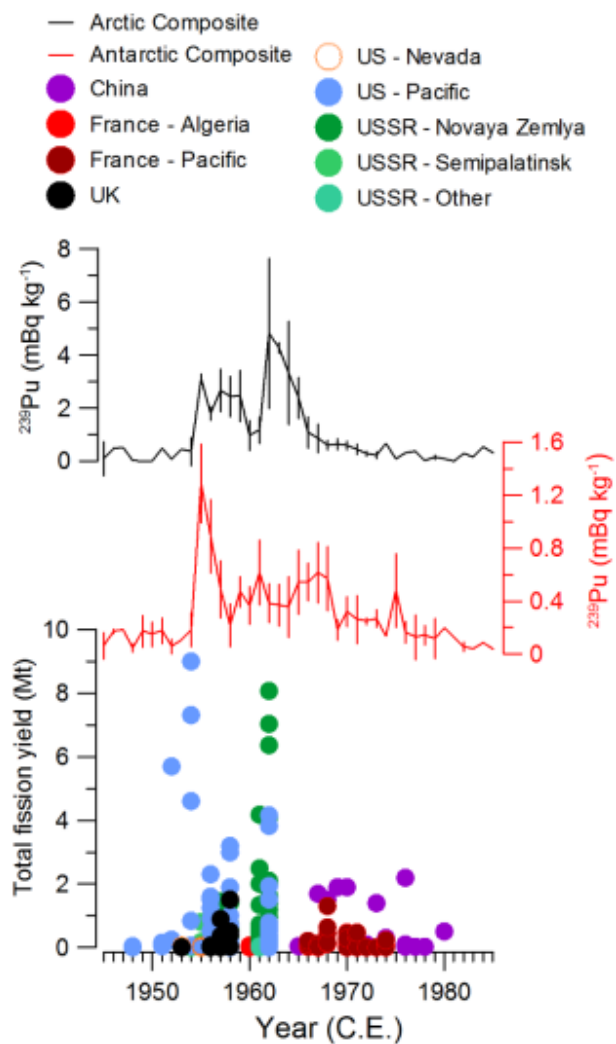
383 Figure 3: Annual average  $^{239}\text{Pu}$  results from the Arctic ice cores with well-constrained ages. (a)  
 384 Semi-quantitative  $^{239}\text{Pu}$  activities and (b) semi-quantitative  $^{239}\text{Pu}$  activity fluxes for each of the  
 385 ice cores with the composite geometric mean in black.

386



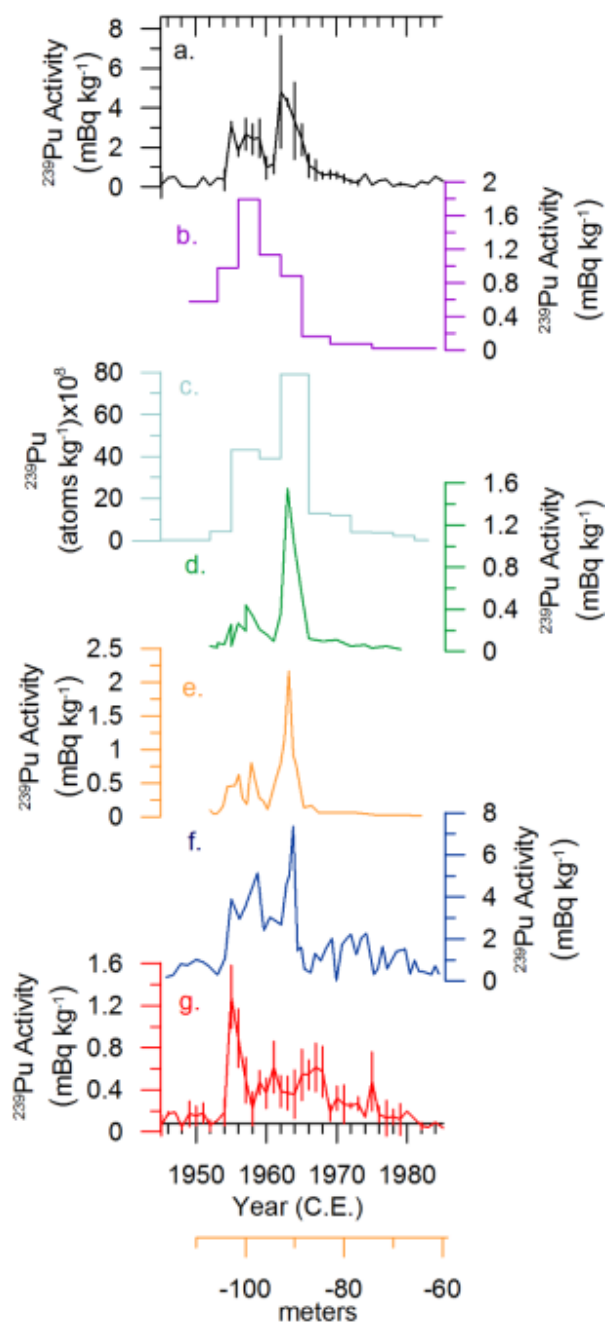
387

388 Figure 4: Annual average  $^{239}\text{Pu}$  results from the Antarctic ice cores with well-constrained ages.  
 389 (a) Semi-quantitative  $^{239}\text{Pu}$  activities and (b) semi-quantitative  $^{239}\text{Pu}$  activity fluxes for each of  
 390 the ice cores with the composite geometric mean in black.



391  
 392 Figure 5: Arctic (black) and Antarctic (red) composite semi-quantitative  $^{239}\text{Pu}$  activity compared  
 393 to total NWT fission yields.<sup>1</sup> The NWT fission yields are divided by country and location of  
 394 testing. Error bars represent the standard error of the mean.

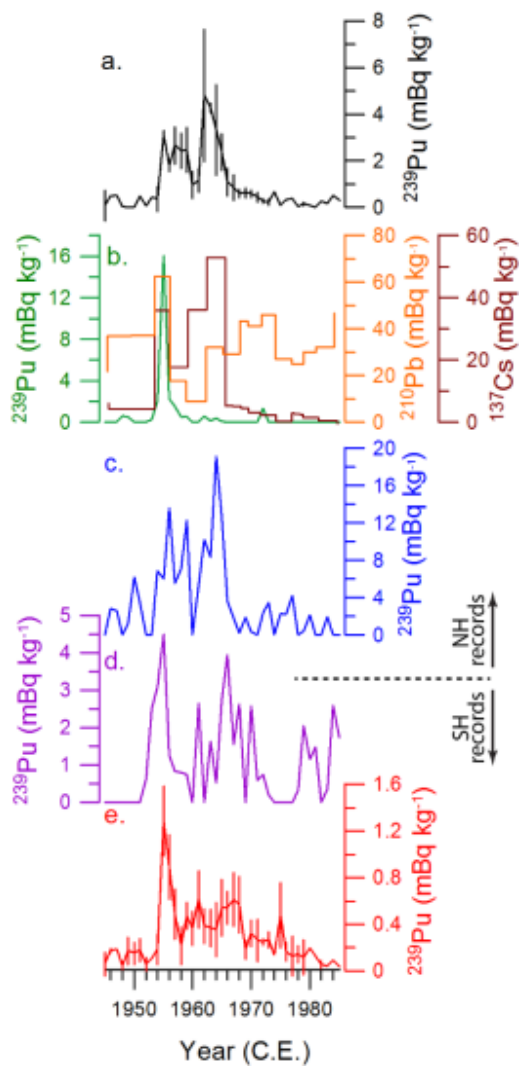
395  
 396  
 397  
 398



399

400 Figure 6: Comparison to previously published  $^{239}\text{Pu}$  records. (a) Arctic mean (this study) (black),  
 401 (b)  $^{239}\text{Pu}$  activity from Austfonna ice core (purple),<sup>2</sup> (c) Belukha Glacier ice core (light blue)<sup>16</sup>,  
 402 (d) herbarium samples collected in the U.K. (green),<sup>4</sup> (e) Colle du Dome ice core (orange),<sup>4</sup> (f)  
 403 Colle Gnifetti ice core (blue),<sup>15</sup> and (g) Antarctic composite (this study) (red). Note the Colle du  
 404 Dome  $^{239}\text{Pu}$  activity record is plotted on its own depth scale. Error bars are standard error of the  
 405 mean.

406



407

408 Figure 7: Comparison between  $^{239}\text{Pu}$  activity records from well-dated ice cores and ice cores  
 409 with less constrained age scales. (a) Arctic composite record, (b) Akademii Nauk ice core  $^{239}\text{Pu}$   
 410 activity (green), (c) McCallUC ice core (blue), (d) the Antarctic NORUS site 8\_5 (purple), and  
 411 (e) the Antarctic composite. Also shown are the Akademii Nauk  $^{210}\text{Pb}$  activity (orange) and  $^{137}\text{Cs}$   
 412 activity (brown) measurements from Pinglot et al.<sup>12</sup> Error bars are standard error of the mean.

413

414

415

416

417

418



419

420 ACKNOWLEDGMENTS

421           The authors would like to thank those who aided with the organization, drilling,  
422 processing and analysis in the field and laboratory. We acknowledge L. Layman for his initial  
423 laboratory work and R. Kreidberg for his editorial advice. The authors would also like to thank  
424 the three anonymous reviewers for their constructive feedback. The following US NSF PLR  
425 grants supported collection and analyses of the cores as well as interpretation of the  
426 measurements: 0538416, 0856845, 0968391, 0909541, 1023672, 1023318, and 1204176. Ice-  
427 core data ( $^{239}\text{Pu}$ ) for all ice cores are accessible at a data repository (to be determined).

428

429

430

431

432

## 433 REFERENCES

- 434 1. UNSCEAR, Annex C: Exposures to the public from man-made sources of radiation. In *Sources*  
435 *and Effects of Ionizing Radiation*, Vienna, 2000.
- 436 2. Wendel, C.; Oughton, D.; Lind, O.; Skipperud, L.; Fifield, L.; Isaksson, E.; Tims, S.; Salbu, B.,  
437 Chronology of Pu isotopes and  $^{236}\text{U}$  in an Arctic ice core. *Science of the Total Environment* **2013**, *461*,  
438 734-741.
- 439 3. Alvarado, J.; Steinmann, P.; Estier, S.; Bochud, F.; Haldimann, M.; Froidevaux, P.,  
440 Anthropogenic radionuclides in atmospheric air over Switzerland during the last few decades. *Nature*  
441 *Communications* **2014**, *5*, (3030), 1-6.
- 442 4. Warneke, T.; Croudace, I.; Warwick, P.; Taylor, R., A new ground-level fallout record of  
443 uranium and plutonium isotopes for northern temperate latitudes. *Earth and Planetary Science Letters*  
444 **2002**, *203*, (3-4), 1047-1057.
- 445 5. Hardy, E.; Krey, P.; Volchok, H., Global inventory and distribution of fallout Plutonium. *Nature*  
446 **1973**, *241*, (5390), 444-445.
- 447 6. Roos, P.; Holm, E.; Persson, R.; Aarkrog, A.; Nielsen, S., Deposition of  $^{210}\text{Pb}$ ,  $^{137}\text{Cs}$ ,  $^{239+240}\text{Pu}$ ,  
448  $^{238}\text{Pu}$ , and  $^{241}\text{Am}$  in the Antarctic Peninsula area. *Journal of Environmental Radioactivity* **1994**, *24*, 235--  
449 251.
- 450 7. Benninger, L.; Dodge, R., Fallout plutonium and natural radionuclides in annual bands of the  
451 coral *Montastrea annularis*, St. Croix, U.S. Virgin Islands. *Geochimica Et Cosmochimica Acta* **1986**, *50*,  
452 (12), 2785-2797.
- 453 8. Lindahl, P.; Asami, R.; Iryu, Y.; Worsfold, P.; Keith-Roach, M.; Choi, M., Sources of plutonium  
454 to the tropical Northwest Pacific Ocean (1943-1999) identified using a natural coral archive. *Geochimica*  
455 *Et Cosmochimica Acta* **2011**, *75*, (5), 1346-1356.
- 456 9. Wendel, C.; Fifield, L.; Oughton, D.; Lind, O.; Skipperud, L.; Bartnicki, J.; Tims, S.; Hoibraten,  
457 S.; Salbu, B., Long-range tropospheric transport of uranium and plutonium weapons fallout from  
458 Semipalatinsk nuclear test site to Norway. *Environment International* **2013**, *59*, 92-102.
- 459 10. Pennington, W.; Tutin, T. G.; Cambray, R. S.; Fisher, E. M., Observations on lake sediments  
460 using fallout  $^{137}\text{Cs}$  as a tracer. *Nature* **1973**, *242*, (5396), 324-326.
- 461 11. Koide, M.; Bertine, K.; Chow, T.; Goldberg, E., The  $^{240}\text{Pu}/^{239}\text{Pu}$  ratio, a potential  
462 geochronometer. *Earth and Planetary Science Letters* **1985**, *72*, (1), 1-8.
- 463 12. Pinglot, J.; Vaikmae, R.; Kamiyama, K.; Igarashi, M.; Fritzsche, D.; Wilhelms, F.; Koerner, R.;  
464 Henderson, L.; Isaksson, E.; Winther, J.; Van de Wal, R.; Fournier, M.; Bouisset, P.; Meijer, H., Ice cores  
465 from Arctic sub-polar glaciers: chronology and post-depositional processes deduced from radioactivity  
466 measurements. *Journal of Glaciology* **2003**, *49*, (164), 149-158.
- 467 13. Elmore, D.; Tubbs, L.; Newman, D.; Ma, X.; Finkel, R.; Nishizumi, K.; Beer, J.; Oeschger, H.;  
468 Andree, M.,  $^{36}\text{Cl}$  bomb pulse measured in a shallow ice core from Dye-3, Greenland. *Nature* **1982**, *300*,  
469 (5894), 735-737.
- 470 14. Kotzer, T. G.; Kudo, A.; Zheng, J.; Workman, W., Natural and anthropogenic levels of tritium in  
471 a Canadian Arctic ice core, Agassiz Ice Cap, Ellesmere Island, and comparison with other radionuclides.  
472 *Journal of Glaciology* **2000**, *46*, (152), 35-40.
- 473 15. Gabrieli, J.; Cozzi, G.; Vallelonga, P.; Schwikowski, M.; Sigl, M.; Eickenberg, J.; Wacker, L.;  
474 Boutron, C.; Gaggeler, H.; Cescon, P.; Barbante, C., Contamination of Alpine snow and ice at Colle  
475 Gnifetti, Swiss/Italian Alps, from nuclear weapons tests. *Atmospheric Environment* **2011**, *45*, (3), 587-  
476 593.
- 477 16. Olivier, S.; Bajo, S.; Fifield, L.; Gaggeler, H.; Papina, T.; Santschi, P.; Schotterer, U.;  
478 Schwikowski, M.; Wacker, L., Plutonium from global fallout recorded in an ice core from the Belukha  
479 glacier, Siberian Altai. *Environmental Science & Technology* **2004**, *38*, (24), 6507-6512.
- 480 17. Schwikowski, M.; Brutsch, S.; Gaggeler, H.; Schotterer, U., A high-resolution air chemistry  
481 record from an Alpine ice core: Fiescherhorn glacier, Swiss Alps. *Journal of Geophysical Research-*  
482 *Atmospheres* **1999**, *104*, (D11), 13709-13719.

- 483 18. Naftz, D.; Klusman, R.; Michel, R.; Schuster, P.; Reddy, M.; Taylor, H.; Yanosky, T.;  
484 McConnaughey, E., Little Ice Age evidence from a south-central North America ice core, USA. *Arctic*  
485 *and Alpine Research* **1996**, *28*, (1), 35-41.
- 486 19. Knusel, S.; Ginot, P.; Schotterer, U.; Schwikowski, M.; Gaggeler, H.; Francou, B.; Petit, J.;  
487 Simoes, J.; Taupin, J., Dating of two nearby ice cores from the Illimani, Bolivia. *Journal of Geophysical*  
488 *Research-Atmospheres* **2003**, *108*, (D6), 1-11.
- 489 20. Fourre, E.; Jean-Baptiste, P.; Dapoigny, A.; Baumier, D.; Petit, J.; Jouzel, J., Past and recent  
490 tritium levels in Arctic and Antarctic polar caps. *Earth and Planetary Science Letters* **2006**, *245*, (1-2),  
491 56-64.
- 492 21. McConnell, J.; Lamorey, G.; Lambert, S.; Taylor, K., Continuous ice-core chemical analyses  
493 using Inductively Coupled Plasma Mass Spectrometry. *Environmental Science & Technology* **2002**, *36*,  
494 (1), 7-11.
- 495 22. Sigl, M.; Winstrup, M.; McConnell, J.; Welten, K.; Plunkett, G.; Ludlow, F.; Büntgen, U.;  
496 Caffee, M.; Chellman, N.; Dahl-Jensen, D.; Fischer, H.; Kipfstuhl, S.; Kostick, C.; Maselli, O.; Mekhaldi,  
497 F.; Mulvaney, R.; Muscheler, R.; Pasteris, D.; Pilcher, J.; Salzer, M.; Schüpbach, S.; Steffensen, J.;  
498 Vinther, B.; Woodruff, T., Timing and climate forcing of volcanic eruptions for the past 2,500 years.  
499 *Nature* **2015**, *523*, 543-549.
- 500 23. Sigl, M.; Ferris, D.; Fudge, T. J.; Winstrup, M.; Cole-Dai, J.; McConnell, J. R.; Taylor, K. C.;  
501 Welten, K.; Woodruff, T. E.; Adolphi, F.; Brook, E. J.; Buizert, C.; Caffee, M. W.; Dunbar, N.; Geng, L.;  
502 Iverson, N.; Koffman, B.; Maselli, O. J.; McGwiew, K.; Muscheler, R.; Nishiizumi, K.; Pasteris, D. R.;  
503 Rhodes, R. H.; Sowers, T.; Svensson, A., The WAIS Divide deep ice core WD2014 chronology - Part 2:  
504 Annual-layer counting (0-31 ka BP). *Climate of the Past Discussions* **2015**, *11*, 3425-3474.
- 505 24. McConnell, J.; Edwards, R.; Kok, G.; Flanner, M.; Zender, C.; Saltzman, E.; Banta, J.; Pasteris,  
506 D.; Carter, M.; Kahl, J., 20th-century industrial black carbon emissions altered Arctic climate forcing.  
507 *Science* **2007**, *317*, (5843), 1381-4.
- 508 25. McConnell, J.; Maselli, O.; Sigl, M.; Vallelonga, P.; Neumann, T.; Anschutz, H.; Bales, R.;  
509 Curran, M.; Das, S.; Edwards, R.; Kipfstuhl, S.; Layman, L.; Thomas, E., Antarctic-wide array of high-  
510 resolution ice core records reveals pervasive lead pollution began in 1889 and persists today. *Scientific*  
511 *Reports* **2014**, *4*, 1-5.
- 512 26. Mulvaney, R.; Abram, N.; Hindmarsh, R.; Arrowsmith, C.; Fleet, L.; Triest, J.; Sime, L.;  
513 Alemany, O.; Foord, S., Recent Antarctic Peninsula warming relative to Holocene climate and ice-shelf  
514 history. *Nature* **2012**, *489*, (7414), 141-U204.
- 515 27. Criscitiello, A.; Das, S.; Karnauskas, K.; Evans, M.; Frey, K.; Joughin, I.; Steig, E.; McConnell,  
516 J.; Medley, B., Tropical Pacific influence on the source and transport of marine aerosols to West  
517 Antarctica. *Journal of Climate* **2014**, *27*, (3), 1343-1363.
- 518 28. Pasteris, D.; McConnell, J.; Edwards, R., High-resolution, continuous method for measurement of  
519 acidity in ice cores. *Environmental Science & Technology* **2012**, *46*, (3), 1659-1666.
- 520 29. Baglan, N.; Cossonnet, C.; Pitet, P.; Cavadore, D.; Exmelin, L.; Berard, P., On the use of ICP-MS  
521 for measuring plutonium in urine. *Journal of Radioanalytical and Nuclear Chemistry* **2000**, *243*, (2), 397-  
522 401.
- 523 30. Koide, M.; Goldberg, E.; Herron, M.; Langway, C., Transuranic depositional history in South  
524 Greenland firn layers. *Nature* **1977**, *269*, (5624), 137-139.
- 525 31. Koide, M.; Michel, R.; Goldberg, E.; Herron, M.; Langway, C., Characterization of radioactive  
526 fallout from pre-moratorium and post-moratorium tests to polar ice caps. *Nature* **1982**, *296*, (5857), 544-  
527 547.
- 528 32. Koide, M.; Goldberg, E.,  $^{241}\text{Pu}/^{239+240}\text{Pu}$  ratios in polar glaciers. *Earth and Planetary Science*  
529 *Letters* **1981**, *54*, (2), 239-247.
- 530 33. Koide, M.; Michel, R.; Goldberg, E.; Herron, M.; Langway, C., Depositional history of artificial  
531 radionuclides in the Ross Ice Shelf, Antarctica. *Earth and Planetary Science Letters* **1979**, *44*, 205-223.
- 532 34. Cutter, G.; Bruland, K.; Risebrough, R., Deposition and accumulation of plutonium isotopes in  
533 Antarctica. *Nature* **1979**, *279*, (5714), 628-629.

- 534 35. Nolan, M.; Arendt, A.; Rabus, B.; Hinzman, L.; Dowdeswell, J.; Willis, I., Volume change of  
535 McCall Glacier, Arctic Alaska, USA, 1956-2003. *Annals of Glaciology, Vol 42, 2005* **2005**, 42, 409-416.
- 536 36. Fritzsche, D.; Wilhelms, F.; Savatyugin, L.; Pinglot, J.; Meyer, H.; Hubberten, H.; Miller, H., A  
537 new deep ice core from Akademii Nauk ice cap, Severnaya Zemlya, Eurasian Arctic: first results. *Annals*  
538 *of Glaciology, Vol 35* **2002**, 35, 25-28.
- 539 37. Pasteris, D.; McConnell, J.; Edwards, R.; Isaksson, E.; Albert, M., Acidity decline in Antarctic  
540 ice cores during the Little Ice Age linked to changes in atmospheric nitrate and sea salt concentrations.  
541 *Journal of Geophysical Research-Atmospheres* **2014**, 119, (9), 5640-5652.

542

543